

IFT-7/99  
 UCD-99-9  
 June, 1999

## Testing Top-Quark Yukawa Interactions in $e^+e^- \rightarrow t\bar{t}$

Bohdan Grzadkowski<sup>1</sup> and Jacek Pliszka<sup>2</sup>

Institute of Theoretical Physics, Warsaw University, Warsaw, Poland  
 and  
 Davis Institute for High Energy Physics, UC Davis, CA, USA

### Abstract

Determination of the top-quark Yukawa couplings in the process  $e^+e^- \rightarrow t\bar{t}$  has been studied for the high luminosity option ( $\mathcal{L} = 500 \text{ fb}^{-1}$ ) of a linear  $e^+e^-$  collider. Polarization of the electron beam has been considered. The method of optimal observables has been adopted to determine the couplings and to disentangle different models. It has been found that it could be possible to discriminate between the Standard Model scalar Higgs boson, pure pseudoscalar and the Higgs boson of mixed CP at about 12% level for  $\sqrt{s} = 1 \text{ TeV}$  for the Higgs boson close to the production threshold both for the leptonic and hadronic top-quark decay channels. However,  $\sqrt{s} = 0.5 \text{ TeV}$  collider turned out to have too small energy for tests of the top-quark Yukawa coupling because of its limited production rate (at most 2.5 events). Possible tests of CP violation in the scalar sector have been considered.

---

<sup>1</sup>E-mail: bohdang@fuw.edu.pl

<sup>2</sup>E-mail: pliszka@fuw.edu.pl

# 1 Introduction

It will be very important to directly determine the Yukawa couplings (and therefore CP nature) of any Higgs boson that would be discovered. Although it is very plausible that a substantial number of Higgs boson events will first be available at the LHC, however future linear  $e^+e^-$  colliders (NLC) could provide much more efficient laboratory to determine couplings of any observed Higgs. The Standard Model (SM) predicts an existence of a scalar Higgs boson, however a pseudoscalar admixture is absolutely conceivable and as leading to renormalizable interactions, it may couple as strongly as the scalar Higgs boson. Since Yukawa couplings are proportional to the appropriate fermion masses, obviously the most promising coupling to study is the one of the top quark. Here, we are going to discuss a possibility to test the top-quark Yukawa coupling in the process  $e^+e^- \rightarrow ttZ$ , our goal will be to estimate what would be the future precision for discrimination between CP-conserving (scalar and pseudoscalar) and CP-violating Yukawa interactions.

For our analysis, the relevant part of the interaction Lagrangian takes the following form :

$$\mathcal{L} = \frac{m_t}{v} h t(a + i_5 b) t + c \frac{g m_Z}{2 \cos \theta_w} h Z Z ; \quad (1)$$

where  $g$  is the SU(2) coupling constant,  $v$  is the Higgs boson vacuum expectation value (with the normalization adopted here such that  $v = 2m_W/g = 246 \text{ GeV}$ )  $a$ ,  $b$  and  $c$  are parameters which account for possible deviations from the SM ( $a = 1$ ,  $b = 0$  and  $c = 1$  reproduce the SM Lagrangian). Since under CP  $t(a + i_5 b) t \xrightarrow{CP} t(a - i_5 b) t$  and  $Z Z \xrightarrow{CP} Z Z$  one can observe that terms in the cross section proportional to  $ab$  or  $bc$  would indicate CP violation. Since for the process considered here ( $e^+e^- \rightarrow ttZ$ ) there are no  $ab$ <sup>11</sup> terms we will focus here on  $bc$  terms. It should be emphasized that this is not just  $bc$  term but also  $(bc)^2$  which are signals of CP violation.

The minimal extension of the SM which provides non-zero  $b$  and  $a; c \neq 1$  is the two-Higgs-doublet model [1] (2HDM). Since the model contains two SU(2) Higgs doublets it could be shown [1] that CP violation may arise in the Higgs sector. Such CP violation is explicit if there is no choice of phases such that all the Higgs-potential parameters are real. However, even if all potential parameters can be chosen to be real, spontaneous CP violation (complex vacuum expectation values) is a possibility. Therefore, the 2HDM is a very attractive and simple model in which to explore the implications of CP violation in the Higgs sector. After SU(2)  $\times$  U(1) gauge symmetry breaking, if either explicit or spontaneous CP violation is present, the three neutral degrees of freedom (one corresponding to the Goldstone boson decouples) mix in the mass matrix and as a result of the mixing between real and imaginary parts of neutral Higgs fields, the Yukawa interactions

<sup>11</sup> Those terms could appear for polarized  $tt$ .

of the mass-eigenstates are not invariant under CP. They are given exactly by form of the Lagrangian defined in Eq.(1). Because of the mixing, the form of the ZZ h coupling will also be modified by the factor c. Both a, b and c are calculable functions of the mixing angles.

Recently, CP violation in a scalar sector has attracted much more attention as it has been realized that it may be generated within the Minimal Supersymmetric Standard Model (MSSM), where due to the CP-violating soft-supersymmetry-breaking Lagrangian complex phases emerge in the effective potential generated at the one-loop level of the perturbation expansion [2]. It turns out that the mixing between the pseudoscalar A and the heavier Higgs boson H can be as large as 25% leading to substantial modification of ZZ h<sub>1</sub> and Zh<sub>1</sub>h<sub>2</sub>, where h<sub>1,2</sub> are the physical mass-eigenstates. Another consequence of the mixing would be CP-violating Yukawa interaction of the form given in Eq.(1).

However, in this paper we are not restricting ourselves to any particular model, on the contrary, our analysis is supposed to be as model independent as possible and we will treat the Lagrangian given by Eq.(1) as an effective interaction.

The process e<sup>+</sup>e<sup>-</sup> → ttZ has been already discussed in the literature by Hagiwara [3] in the context of the SM. Since the total luminosity for the e<sup>+</sup>e<sup>-</sup> linear collider considered there was a factor of 50 lower than the recently discussed in the context of the TESLA project [4] we found it was worth to reconsider the process applying some more elaborate statistical methods to test the Yukawa couplings in the framework of the effective Lagrangian without referring to any given model. Atwood and Soni first noticed in their paper [5] that the process e<sup>+</sup>e<sup>-</sup> → ttZ could be used to test CP violation in the Higgs sector, the advantage of the process is that CP violation appears even at the tree-level approximation of the perturbation expansion. This is why its consequences could be relatively large. However Ref. [5] restricts its discussion to the specific case of the 2HDM what makes its applicability much more limited. We shall compare our results both with Ref. [3] and Ref. [5].

The paper is organized as follows. In Section 2 we will briefly review the method of the optimal observables. Section 3 will contain a description of our strategy and results for the determination of the top-quark Yukawa couplings. Section 4 will be devoted to the summary and conclusions concerning tests of the top-quark Yukawa couplings at the NLC. In the Appendix, an analytic form for the contribution to the matrix element squared linear in the CP-violating couplings will be presented.

## 2 The Optimal Analysis Procedure

We shall consider the process of ttZ production at linear e<sup>+</sup>e<sup>-</sup> colliders:

$$e^+(p_+) + e^-(p_-) \rightarrow t(p_t) + \bar{t}(\bar{p}_t) + Z(k); \quad (2)$$

where momenta of the particles involved have been indicated. Since the electron beam could be relatively easily polarized, besides unpolarized beam we will discuss electrons with positive and negative helicity. The differential cross section for the process could be written in the following way:

$$\frac{d}{d} = f_{VV}^h + acf_{ac} + (ac)^2 f_{(ac)^2} + bcf_{bc} + (bc)^2 f_{(bc)^2}^i; \quad (3)$$

where  $f_{VV}$  stands for non-Higgs contribution, whereas other  $f_i$  are defined through coefficients standing in front of them.  $d$  denotes the final state phase space configuration,  $c$  is the factor which parameterize the  $ZZh$  coupling,  $a$  and  $b$  are the scalar- and pseudoscalar-type Yukawa couplings defined in Eq.(1).

Here, we wish to discriminate between various models on the basis of the difference between the phase space distribution dependence of  $f_{bc}$ ,  $f_{ac}$ ,  $f_{(bc)^2}$  and  $f_{(ac)^2}$ .

In general, for  $d = \sum_i c_i f_i(d)$  (where  $f_i(d)$  are known functions, including normalization) the determination of the unknown signal coefficients  $c_i$  with the smallest possible statistical error is given [6] by

$$c_i = \sum_k M_{ik}^{-1} I_k; \quad \text{where } M_{ik} = \int \frac{f_i(d) f_k(d)}{d} d; \quad \text{and } I_k = \int f_k(d) d; \quad (4)$$

The covariance matrix for the  $c_i$  is

$$V_{ij} = \langle c_i c_j \rangle = \frac{M_{ij}^{-1}}{N} = M_{ij}^{-1} L_e; \quad (5)$$

where  $\tau = \int \frac{d}{d} d$  is the integrated cross section and  $N = L_e \tau$  is the total number of events, with  $L_e$  being the luminosity times the efficiency. This result is the optimum regardless of the relative magnitudes of the different contributions to  $d$ . It is equivalent to determine  $c_i$  by maximizing the likelihood (in the Gaussian statistics limit) of the fit to the full distribution of all the events. The increase in errors due to statistical fluctuations in the presence of background is implicit in the possible background contribution to  $d$  appearing in Eq. (4), which implies larger  $M_{ij}^{-1}$  entries in Eq. (5). From the result of Eq. (5), the  $\chi^2$  in the  $c_i$  parameter space is then computed as

$$\chi_X^2(Y) = \sum_{ij} (c_i^0 - c_i) V_{ij}^{-1} (c_j^0 - c_j) = \sum_{ij} (c_i^0 - c_i) L_e M_{ij} (c_j^0 - c_j); \quad (6)$$

where, for our theoretical analyses, the  $c_i$  and  $V_{ij}$  are computed within the model  $X$ , while  $c_i^0$  should be calculated for the model  $Y$  tested against the model  $X$ . The value of  $\chi_X^2(Y)$  indicates how well could one distinguish  $X$  and  $Y$ . The power of the optimal analysis technique is to take full advantage of all the information available in the cross section as a function of the kinematical variables.

The above procedure is not altered if cuts are imposed on the kinematical phase space over which one integrates; one simply restricts all integrals to the accepted region. If a subset,  $\Omega$ , of the kinematical variables cannot be determined, then the optimal technique can be applied using the variables,  $\hat{\Omega}$ , that can be observed and the functions  $f_i(\hat{\Omega}) = \int_{\Omega} f_i(\Omega) d\Omega$ .

### 3 Strategy and Results

Feynman diagrams describing the process  $e^+e^- \rightarrow ttZ$  are shown in Fig.1. One can think about the process considered here as a way to measure the top-quark Yukawa interaction of a Higgs boson produced in a strahlung process of the Z line  $e^+e^- \rightarrow Zh$  followed by the decay  $h \rightarrow tt$ . However, here we allow also for Higgs boson being on-shell, see the diagram (a) in Fig.1. Within this interpretation the remaining (purely SM-type) diagrams (b), (c), (d) and (e) describe a continuum background for the Higgs boson decaying to tt pair. Since we are trying to determine the top-quark Yukawa coupling the contribution to the matrix element squared relevant for us would be the interference of the Higgs-boson-exchange diagram (a) with Z-boson radiation of top-quark line<sup>12</sup> (d), (e) and the square of the Higgs diagram (a). In some sense the process  $e^+e^- \rightarrow ttZ$  considered here is complementary to  $e^+e^- \rightarrow tth$  discussed recently in Ref.[7], as both processes originate from the Higgs-boson strahlung of Z line followed either by  $h \rightarrow tt$  or  $Z \rightarrow tt$ , respectively.

Before we start the optimal analysis it is useful to recollect the SM predictions for the total Higgs-boson width  $\Gamma_h^{SM}$  and also the total cross section for the process of interest ( $e^+e^- \rightarrow ttZ$ ) for various  $\sqrt{s}$  and Higgs-boson masses  $M_h$ , for polarized  $j = \pm 1$  and unpolarized  $j = 0$  electron beams. Results are presented in Fig.2<sup>13</sup>. Because the Higgs boson could be on its mass shell, the Breit-Wigner form of the propagator must be adopted, therefore it is relevant to remind ourselves the strong increase of  $\Gamma_h$  as a function of  $M_h$ , see plot (a) in Fig.2. Concerning the total cross section as a function of  $\sqrt{s}$  we observe a threshold increase at  $\sqrt{s} = m_Z + 2m_t$  followed by a typical s-channel suppression for higher energies. For the polarization dependence, the relative suppression of the polarization  $j = \pm 1$  could have been anticipated, as it is caused by a constructive and destructive interference between  $\gamma$  and Z exchange diagrams for  $j = \pm 1$  and  $j = 0$ , respectively. As it is seen from plots (c) and (d) in Fig.2 the relative contribution from the Higgs boson to the total cross section could reach up to 30% in the threshold region. It could be read from Fig.2 that for a given  $\sqrt{s}$  the total cross section for low Higgs-boson mass,

<sup>12</sup>The interference of the Higgs-boson-exchange Feynman diagram with Z radiation of the initial electron line vanishes.

<sup>13</sup>Using our code we have obtained exactly the results presented for the SM by Hagiwara et al. in Ref. [3]. Other test we have performed was to reproduce the narrow-width approximation for the on-shell Higgs boson. We have also checked our code against the analytical form shown in the Appendix for the contribution linear in bc.

$M_h = 200$ , is greater than the one for high mass. That means that the Higgs-boson-exchange diagram (a) adds constructively with the other diagrams for low masses and interferes destructively in the region of high masses. In fact, it is seen from Fig. 3 where separate contributions to  $\sigma_{\text{tot}}(e^+e^- \rightarrow ttZ)$  have been plotted. This is related to the correct high-energy behavior of the cross section in the large  $M_h$  limit. Since the virtual Z boson couples to massless electrons, effectively it is mostly the transverse component which propagates and therefore the Higgs-boson exchange is not necessary to provide "good" high-energy behavior in the infinite Higgs-boson mass limit.<sup>14</sup> Quantitatively however, the effect is totally negligible for the total cross section.

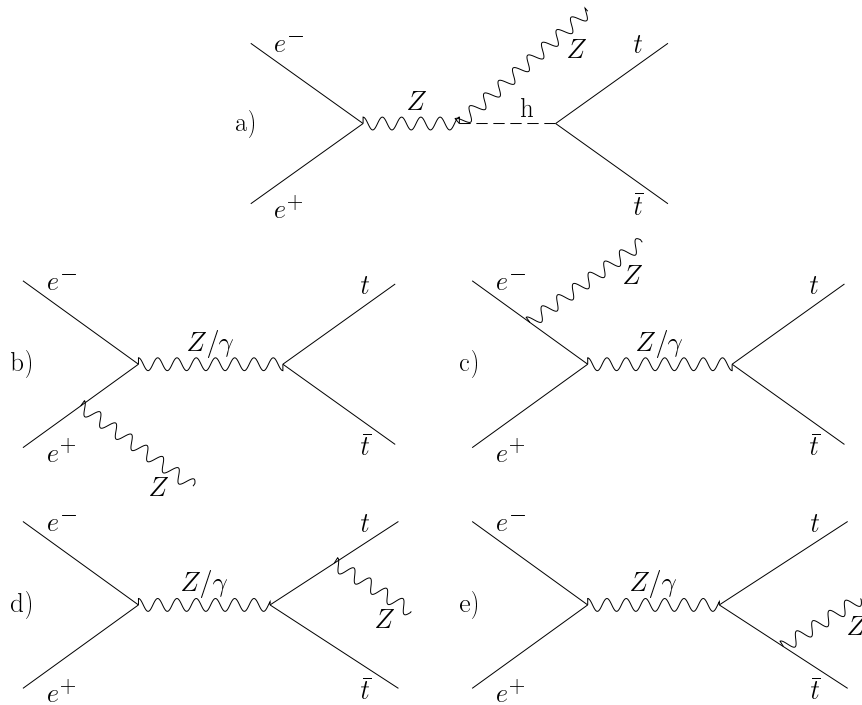


Figure 1: The Feynman diagrams for the process  $e^+e^- \rightarrow ttZ$ .

Following detector design of the Japanese Linear Collider [8] we impose here the polar angle cut  $|\cos \theta| < 0.98$ . We will consider separately two cases. For the first one, which we call the leptonic case, one top quark decays hadronically and the other leptonically and the second one, which we call the hadronic case in which both  $t$  and  $\bar{t}$  decay hadronically. We choose the following  $tt$  tagging efficiencies: 30% for leptonic and 44% for hadronic modes. For hadronic decays it is very difficult to disentangle experimentally  $t$  and  $\bar{t}$ , we would be only able to tell from the invariant mass reconstruction that a given jet corresponds to  $t$  or  $\bar{t}$ . Therefore, adopting the optimal observables for hadronic  $tt$  decays, we will

<sup>14</sup>For a detailed discussion of unitarity constraints see Ref. [3].

always be averaging over  $t$  and  $\bar{t}$  that would correspond to  $t$  and  $\bar{t}$  tagging just by the invariant mass measurement without determining the charge of decaying top quarks. Obviously, for leptonic decays it is not necessary since the charge of hadronically decaying top quark would be identified by the lepton charge from the semileptonic decay of the other top quark. For simplicity we will assume 100% efficiency for  $Z$  tagging. For definiteness, in what follows, we will consider one year of operation for high luminosity option of the NLC that has been examined in the context of the TESLA collider design, for which one expects  $\mathcal{L} = 500 \text{ fb}^{-1} \text{ y}^{-1}$ . [4].

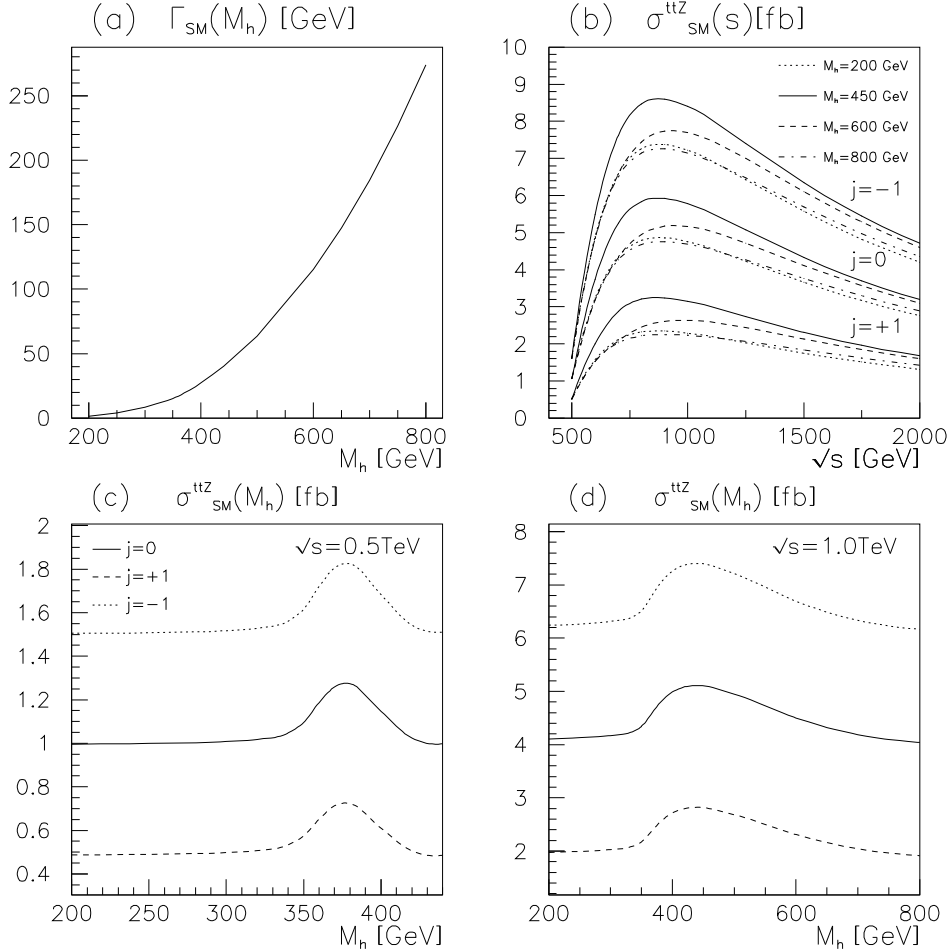


Figure 2: The SM predictions for the total Higgs-boson width (a), the total cross section for  $e^+e^- \rightarrow \text{ttZ}$  for indicated polarization of the initial electron beam ( $j = -1; 0; +1$ ) as a function of  $\sqrt{s}$  for fixed Higgs-boson mass  $M_h$  (b), and the total cross section as a function of  $M_h$  for  $\sqrt{s} = 0.5 \text{ TeV}$  (c) and for  $\sqrt{s} = 1.0 \text{ TeV}$  (d).

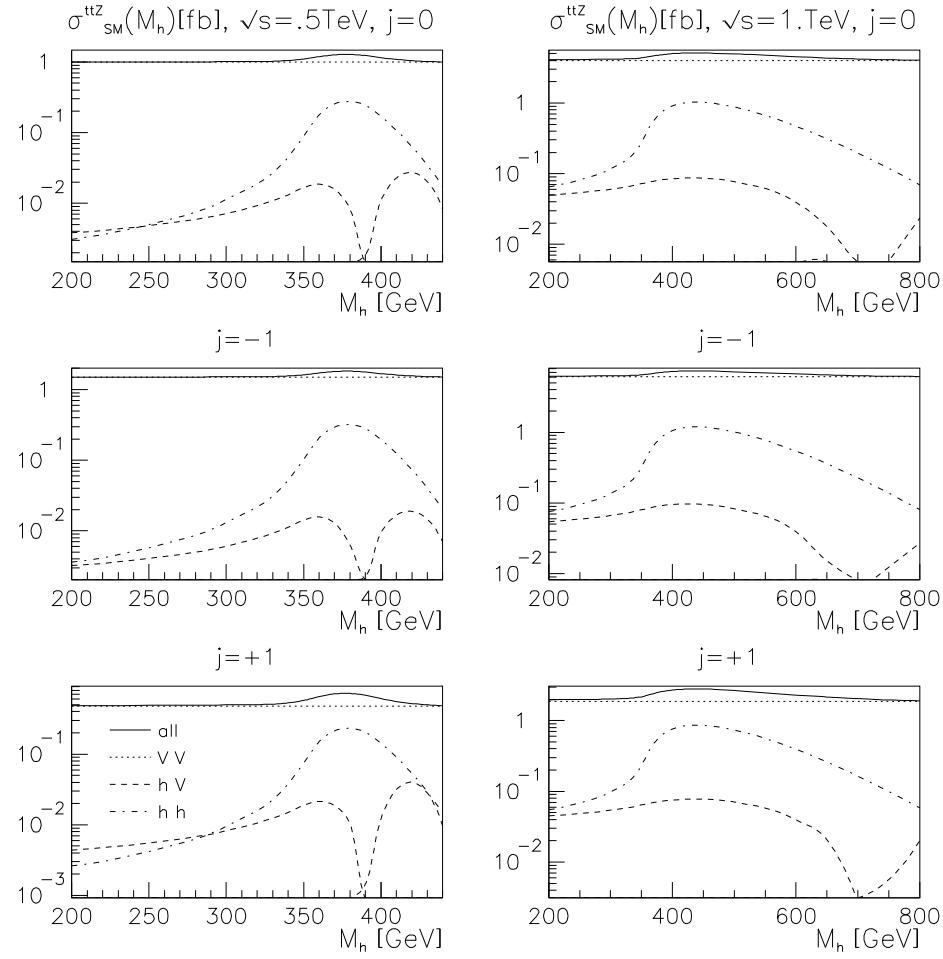


Figure 3: The SM predictions for the total cross section for  $e^+e^- \rightarrow ttZ$  for indicated polarization of the initial electron beam ( $j = 1; 0; +1$ ) as a function of Higgs-boson mass  $M_h$  for  $\sqrt{s} = 0.5 \text{ TeV}$  and for  $\sqrt{s} = 1 \text{ TeV}$ . Contributions from the Higgs-boson diagram squared ( $hh$ ), all non-Higgs diagrams ( $VV$ ), and from the interference between Higgs and non-Higgs diagrams ( $hV$ ) have been plotted separately. The interference becomes negative for  $M_h > 390 \text{ GeV}$  and  $700 \text{ GeV}$  at  $\sqrt{s} = 0.5 \text{ TeV}$  and  $\sqrt{s} = 1 \text{ TeV}$ , respectively. Therefore we have plotted the absolute value of the interference term. The solid line stands for the sum of all the contributions.

We first focus on the detection of CP violation in the process  $e^+e^- \rightarrow ttZ$ . As has already been mentioned CP, violation would result in the appearance of non-zero  $bc$  and  $(bc)^2$  terms in the differential distribution, Eq.(3). An interference of the Higgs-exchange Feynman diagram with the Z radiation on the final top-quark lines generates terms  $bc$ , whereas  $(bc)^2$  are emerging from the square of the Higgs-exchange diagram. Let us assume that the non-standard CP-odd admixture to the Yukawa coupling is small, so that the terms proportional to  $(bc)^2$  could be neglected and the leading contribution is the one linear in  $bc$ . In the Appendix we present the analytical formula for the contributions to the matrix element squared that are proportional to  $bc$ . It turns out that in the small  $bc$  limit the differential cross section could be written in the form  $(\sigma) = \sum_i c_i f_i(\dots)$  and the optimal analysis

outlined in the previous section could be directly applicable<sup>15</sup>.

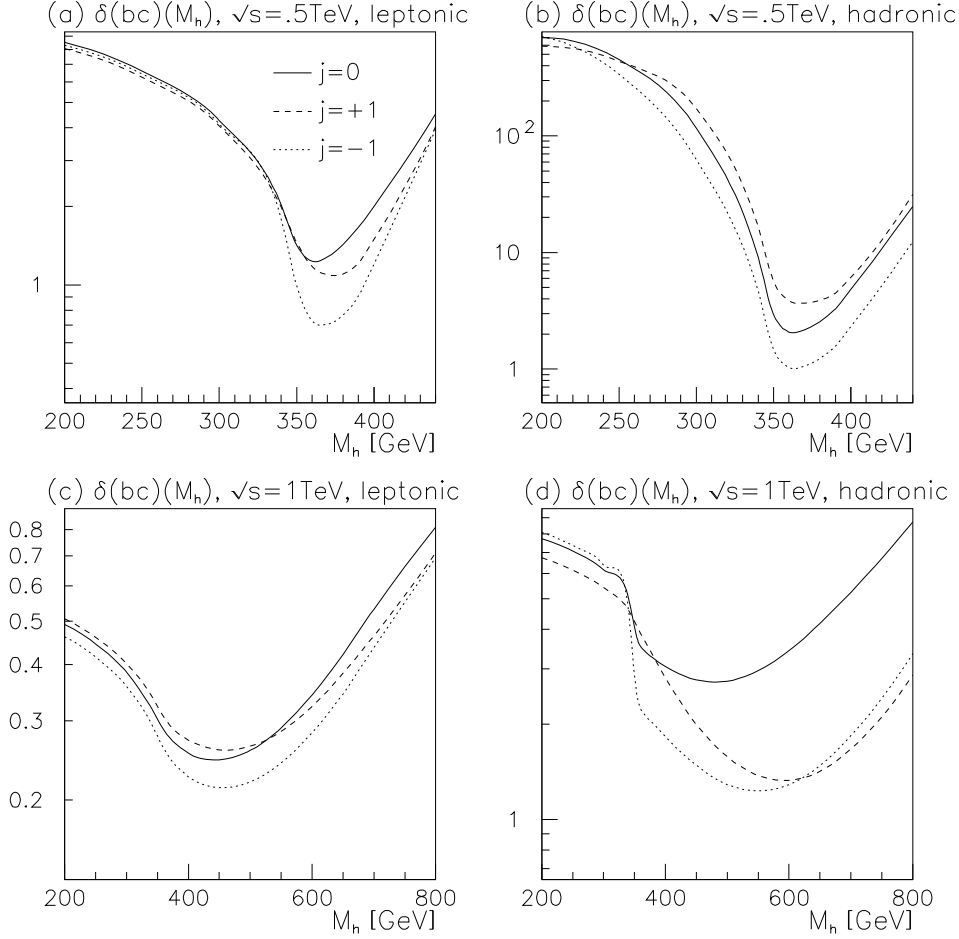


Figure 4: The statistical error  $\delta(bc)$  for the determination of  $bc$  for the case when  $(bc)^2$  could be neglected, calculated for the indicated polarizations of the initial electron beam and  $\sqrt{s} = 0.5; 1\text{TeV}$ .

As it has been shown in Ref. [6] one can construct an appropriate weighting function  $w_i(\vec{c})$  such that  $\int w_i(\vec{c}) \mathcal{P}(\vec{c}) d\vec{c} = c_i$ . The covariance matrix for such observables is given by the Eq.(5). In our simple case when only linear terms in the unknown coupling  $bc$  are kept, the weighting function for determination of  $bc$  and

<sup>15</sup>Notice that the Higgs-boson width  $\Gamma_h$  enters the matrix element squared through the denominator of the Higgs boson propagator. Since  $\Gamma_h$  depends on  $a^2, b^2$  and  $c^2$  the differential cross section is not a polynomial in couplings to be determined, therefore in general Eqs.(4,5) are not applicable. However, for small  $b$  one can expand the propagator around its SM form. Since we are going to keep only linear terms in  $b$ , effectively we are allowed to use the SM form of the propagator while calculating the functions  $f_i$ . Therefore, in the small  $b$  limit, the differential cross section is of the desired form indeed.

its statistical error become:

$$\delta_{bc} = \sqrt{\frac{f_{bc}^2}{N} + \frac{f_{bc}^2}{N} \frac{1}{R}} \quad (7)$$

$$\delta_{bc} = \frac{1}{N} \sqrt{\frac{f_{bc}^2}{R} + \frac{f_{bc}^2}{R} \frac{1}{R}} \quad ; \quad (8)$$

where  $\delta_{bc}$  denotes SM contribution to the differential cross section. Numerical results for  $\delta_{bc}$  are shown in Fig. 4. As seen from the figure, the smallest errors appear for  $M_h$  such that the Higgs boson could be on its mass shell and decay to  $t\bar{t}$ , this is the region corresponding to the maximal cross section, see Fig. 2. In general, hadronic top-quark decay modes provide much larger errors, however in the vicinity of  $M_h = 370$  GeV both hadronic and leptonic final states lead to errors of the order of 1: for  $\sqrt{s} = 5$  TeV. For  $\sqrt{s} = 1$ : TeV minimal errors are obtained for  $M_h = 450$  GeV for leptonic decays and one can see that leptonic modes over  $\delta_{bc} \sim 25$  whereas for the hadronic ones we get  $\delta_{bc} > 1$ . The enhancement of the error for the hadronic modes illustrates how important the  $t\bar{t}$  identification is. As expected, losing information on the top-quark charge leads to larger errors.

Let us now consider the general case with non-negligible terms  $O(\delta^2)$ . Then the dependence of the differential distribution Eq.(3) on the unknown couplings  $a$ ,  $b$  and  $c$  is much more involved since the Higgs-boson width, which enters the denominator of the Higgs-boson propagator also depends on those couplings. In other words, functions  $f_i$  appearing in the distribution shown in Eq.(3) are unknown as being  $a$ ,  $b$  and  $c$  dependent. However, we shall assume here that at the time when the NLC will operate the total Higgs-boson width  $\Gamma_h$  will be known from measurements at the LHC. Therefore we are going to consider only those extensions to the SM that predict the same  $\Gamma_h$ , otherwise the model would be experimentally excluded at the very beginning. Moreover, the measurement of the total cross section for the process  $e^+e^- \rightarrow t\bar{t}Z$  would also eliminate those models for which the cross section would differ from the measured one. Therefore, in addition, we will restrict ourselves to those models which provide the total cross section identical with the SM one<sup>16</sup>. The models we are discussing are specified by the couplings  $a$ ,  $b$  and  $c$  appearing in the Lagrangian given by Eq.(1), the following versions will be considered:

$$\text{SM} : a = 1, b = 0, c = 1$$

$$\text{CP-mix.1} : a = b > 0$$

$$\text{CP-mix.2} : a = b < 0$$

$$\text{CP-odd} : a = 0$$

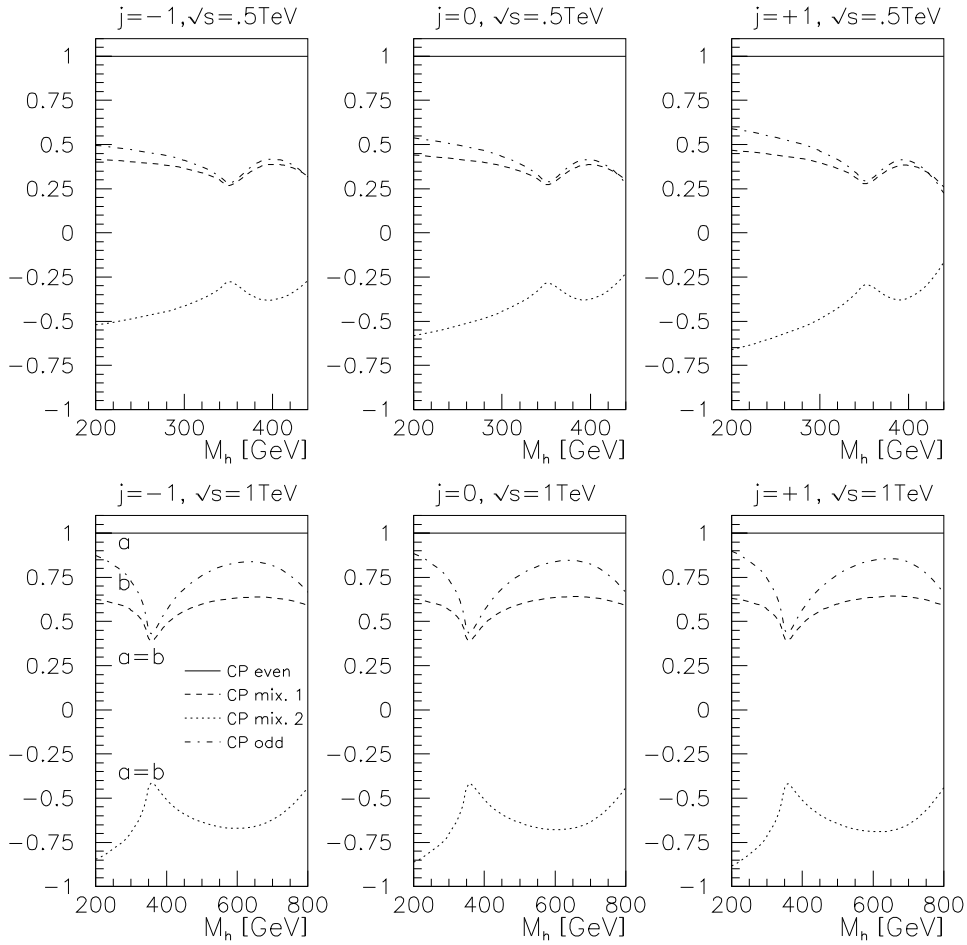


Figure 5: Solutions for  $a$  and  $b$  as a function of the Higgs boson mass. For a given  $M_h$ , plotted  $a$  and  $b$  reproduce SM values for  $\sigma_h$  and  $\sigma_{\text{tot}}(e^+e^- \rightarrow t\bar{t}Z)$  for various polarizations of the initial electron beam.

For given  $M_H$  and  $\sqrt{s}$  values, the width  $\Gamma_h$  and the cross section  $\sigma_{\text{tot}}(e^+e^- \rightarrow t\bar{t}Z)$  could be read directly from Fig. 2. Specific values for  $a$ ,  $b$  and  $c$  for the last three models are obtained by solving the quadratic equations resulting from our requirements of  $\Gamma_h = \Gamma_h^{\text{SM}}$  and  $\sigma_{\text{tot}}(e^+e^- \rightarrow t\bar{t}Z) = \sigma_{\text{tot}}^{\text{SM}}(e^+e^- \rightarrow t\bar{t}Z)$ <sup>17</sup>. As the equations to be solved are quadratic we have several solutions, we have chosen to discuss only those with the value of  $c$  closest to 1. In the CP-mixed case there are both solutions with  $a = b > 0$  and  $a = b < 0$  we chose to discuss both cases. Since

<sup>16</sup>The choice of the SM values for the width and the cross section is, of course, arbitrary. It serves just a possible example of the future experimental data.

<sup>17</sup>It should be mentioned that relaxing this constraint may lead to different conclusions, see Ref. [5], where models corresponding to very distinct  $\Gamma_h$  and  $\sigma_{\text{tot}}(e^+e^- \rightarrow t\bar{t}Z)$  have been compared. We have checked that for models compared in Ref. [5] either widths or total cross sections differ by about a factor of 2.

for all considered models it turns out that  $c$  is very close to 1 (for  $M_h = 100$  GeV we have found  $0.98 < c < 1.05$ , for higher masses  $c = 1 \pm 0.07$ ) we present in Fig. 5 only solutions for  $a$  and  $b$  as a function of  $M_h$ . As it is seen, substantial deviations from the SM are possible keeping  $M_h = M_h^{\text{SM}}$  and  $\sigma_{\text{tot}}(e^+e^- \rightarrow t\bar{t}) = \sigma_{\text{tot}}^{\text{SM}}(e^+e^- \rightarrow t\bar{t})$ . Since the total cross section (see Fig. 2) depends on the initial beam polarization the solutions for  $a$  and  $b$  also vary with the polarization. Kinks in the curves correspond to the region where Higgs-boson contribution to the total cross section for  $\sigma_{\text{tot}}(e^+e^- \rightarrow t\bar{t})$  is maximal, i.e. in the vicinity of the threshold for a real Higgs boson decaying into  $t\bar{t}$ .

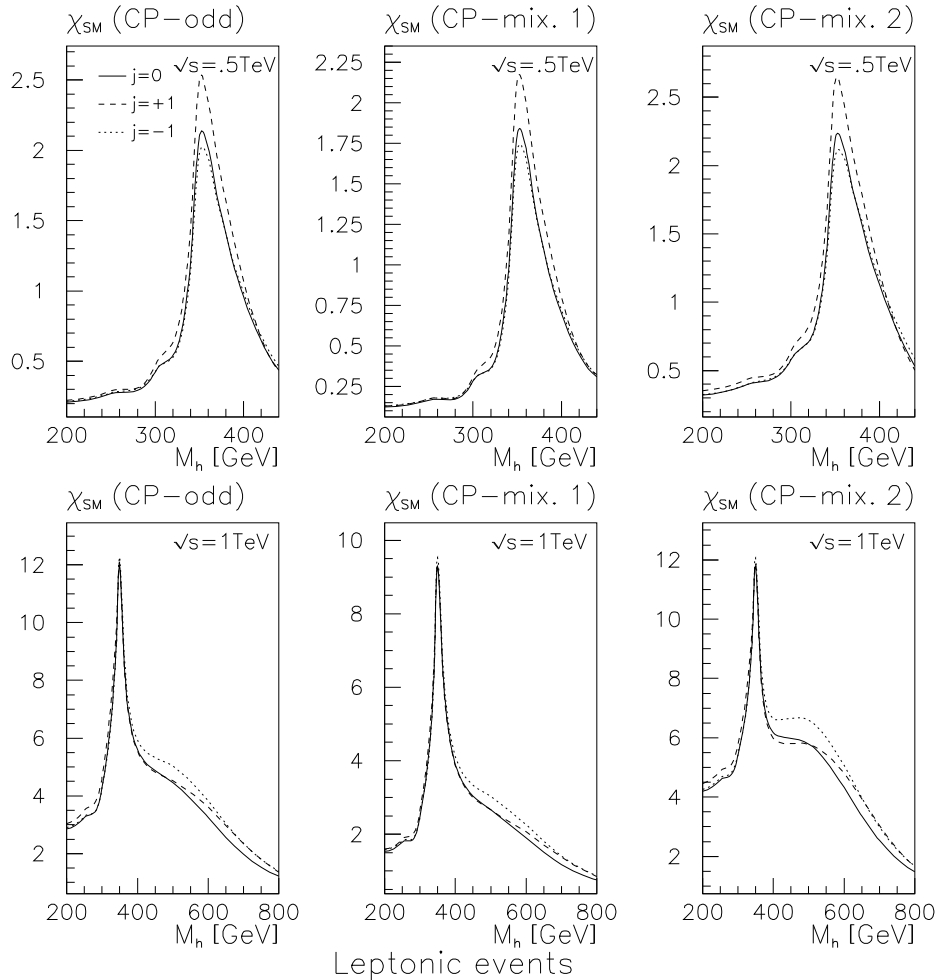


Figure 6:  $\chi_{\text{SM}}(Y) = \frac{\sigma_{\text{SM}}(Y)}{\sigma_{\text{SM}}^{\text{SM}}(Y)}$  where  $\sigma_{\text{SM}}(Y)$  is defined by Eq.(6) calculated for semileptonic top-quark decay final states (at least one  $W$  boson decays leptonically). The models considered are specified in the text. Results are presented for polarized initial electron beams ( $j = -1; 0; +1$ ) and the total energy  $\sqrt{s} = 0.5; 1 \text{ TeV}$ .

Since we stay within a class of models predicting the same  $\sigma_{h, \text{CP odd}}$ <sup>18</sup>, therefore we are entitled to adopt the method of the optimal observables since the functions  $f_i$  from Eq.(3) are known indeed. In Figs. 6 and 7 we show results for  $\sigma_X(Y) \approx \frac{2}{X} \sigma(Y)$  calculated according to Eq.(6) for the leptonic and hadronic events, respectively. First of all we can see that for  $\sqrt{s} = 5 \text{ TeV}$  even in the threshold region  $\sigma$  never exceeds 2:6 both for leptonic and hadronic top-quark decays, making any conclusions very uncertain. The initial electron polarization may be helpful to some extent, although its effect is never very large. For  $\sqrt{s} = 1: \text{TeV}$  we observe for the leptonic events that  $\sigma_{\text{SM}}(\text{CP odd})$  is reaching 12:0 in the vicinity of the threshold and it is above 3:8 up to  $M_h = 600 \text{ GeV}$ . For the hadronic events the maximal  $\sigma$  is more or less the same, however the region of large  $\sigma$  is much more concentrated around the threshold. This should be understood as a consequence of averaging over  $t$  and  $\bar{t}$  as it suppresses contributions from terms linear in  $\cos\theta$  leaving just the contribution from the square of the Higgs-exchange.

It is worth mentioning that even though Fig. 3 was generated for the SM it is, in part, still applicable in the context of the extensions defined above. This is because the constraint  $\sigma_h = \sigma_h^{\text{SM}}$  implies for  $c \neq 1$  that  $\sigma_h(h \rightarrow t\bar{t})$  should also be of the SM size. Therefore, approximately, the contribution from the Higgs-boson diagram squared should be close to the SM one for  $M_h > 2m_t$ <sup>19</sup>. Since  $\sigma_{\text{tot}}(e^+e^- \rightarrow t\bar{t}Z) = \sigma_{\text{tot}}^{\text{SM}}(e^+e^- \rightarrow t\bar{t}Z)$ , it is obvious that the interference between the Higgs and non-Higgs diagrams must also be the same.

One could notice that, in spite of the fact that  $\sigma_{\text{tot}}(j = +1) < \sigma_{\text{tot}}(j = 0) < \sigma_{\text{tot}}(j = -1) < \dots$  there are such models that for certain Higgs-boson masses we have  $\sigma_{\text{tot}}(j = +1) > \sigma_{\text{tot}}(j = 0) > \sigma_{\text{tot}}(j = -1)$ . One should however remember that for a given  $M_h$  the model parameters  $a, b$  and  $c$  adopted for  $j = \pm 1, 0$  are not the same as they are adjusted to reproduce the SM prediction for  $\sigma_h$  and  $\sigma_{\text{tot}}(e^+e^- \rightarrow t\bar{t}Z)$ , see Fig 5. The functions  $f_i$  utilized according to Eq.(4), for the calculation of  $M_{ij}$  are also polarization dependent. In consequence it may happen that the polarization leading to a lower total number of events provides higher  $\sigma$  for certain models.

One could also try to disentangle the CP-odd model and the models of fixed-CP-Yukawa couplings. However it turns out that the  $\sigma_{\text{CP odd}}(\text{CP mix 1})$  is always below 0:4 and 2:3 for  $\sqrt{s} = 5$  and  $1: \text{TeV}$ , respectively. In other words the models are too similar to be distinguished even by the method of optimal observables. As for  $\sigma_{\text{CP odd}}(\text{CP mix 2})$  the maximal values obtained at  $\sqrt{s} = 5$  and  $1: \text{TeV}$  are 1:0 and 6:2, respectively. Leptonic decay modes lead always to higher  $\sigma$ .

So far we have been considering only production of unpolarized  $t\bar{t}$  pairs. However, it is well known that helicity of the top quark could be statistically determined through its semileptonic decay modes, e.g. lepton energy distribution is sensitive

<sup>18</sup>The one measured in the future at LHC. Here it is assumed to be  $\sigma_h^{\text{SM}}$ .

<sup>19</sup>As it is saturated for  $M_h > 2m_t$  by the Higgs-boson resonance contribution:  $\sigma_{\text{tot}}(e^+e^- \rightarrow t\bar{t}Z) \approx \sigma_{\text{tot}}(hZ) \approx \sigma_h(h \rightarrow t\bar{t}) = \sigma_h$

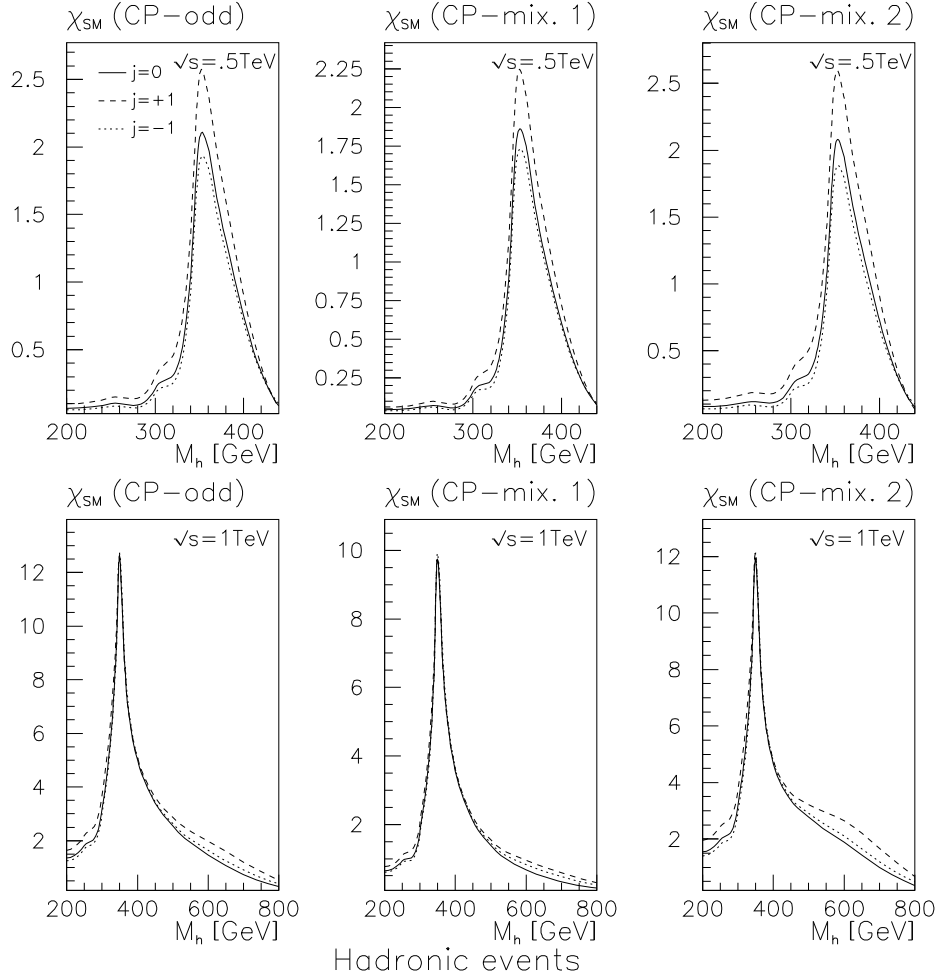


Figure 7:  $\chi_{SM}$  ( $Y$ ) as in Fig. 6 but for purely hadronic top-quark decays.

to the initial top-quark helicity [9]. It is easy to notice that for polarized  $t\bar{t}$  pairs differential distributions would contain, in addition to  $bc$ , also other possible signal of CP violation, namely terms proportional to  $ab$ . To perform a realistic analysis one should consider  $t, \bar{t}$  and  $Z$  decays and then having 8-body final phase space determine  $ab$  and  $bc$  applying the method of optimal observables, this is however beyond the scope of this paper.

## 4 Summary and Conclusions

The method of the optimal observables [6] has been applied to study Yukawa couplings of the top quark in the process  $e^+e^- \rightarrow t\bar{t}Z$ . The high luminosity ( $\mathcal{L} = 500 \text{ fb}^{-1} \text{y}^{-1}$ ) option of linear  $e^+e^-$  colliders examined in the context of the TESLA collider design [4] has been adopted. Using the optimal weighting function  $\omega_{bc}$  given by Eq.(8) we have found that the minimal statistical error for

establishing CP violation in the scalar sector through determination of  $bc$ ,  $(bc)$  could be of the order of  $\pm 25$  for  $M_h \approx 450 \text{ GeV}$  for the  $\sqrt{s} = 1 \text{ TeV}$  collider. The optimal observables have been used to disentangle the SM (CP-even) and CP-odd or CP-mixed Yukawa couplings. In order to make analysis more realistic only models predicting the total Higgs-boson width and the total cross section for  $e^+e^- \rightarrow t\bar{t}Z$  equal to those of the SM have been considered. It turned out that the lower energy option  $\sqrt{s} = 0.5 \text{ TeV}$  of the collider provides too small production rate to be applicable for the determination of the top-quark Yukawa coupling. For  $\sqrt{s} = 1 \text{ TeV}$  one could distinguish the models considered here even at the level of  $\delta = 12$  (for  $M_h \approx 350 \text{ GeV}$ ). However, the results presented in this paper correspond to nearly ideal experimental setup. The full analysis should include background and detector simulation which would not only lower the efficiencies but also, due to the finite detector resolution, would smear both the signal and background distributions. A detailed study including all those effects would be desired. Since the statistical significances found here were relatively large one can believe that in a real experiment it would be possible to determine the top-quark Yukawa coupling at least in the threshold region.

#### Acknowledgments

This work was supported in part by the State Committee for Scientific Research (Poland) under grant No. 2 P 03B 014 14 and by Maria Skłodowska-Curie Joint Fund II (Poland-USA) under grant No. MEN/NSF-96-252. The authors are indebted to the U.C. Davis Institute for High Energy Physics for the great hospitality extended to them while this work has been completed.

## Appendix

Below we present contributions to the matrix element squared which are linear in  $bc$ . As it is seen we have separated terms proportional to the real ( $\text{Re } \Gamma_h$ ) and imaginary ( $\text{Im } \Gamma_h$ ) part of the Higgs-boson propagator  $\Gamma_h(p_h^2) = [\Gamma_h^2 - m_h^2 + i\text{Im } \Gamma_h]^{-1}$  for  $p_h = p_t + p_{\bar{t}}$ :

$$\mathcal{M}_{bc}^2 = bc \frac{g^6 m_t^2}{128 \cos^6 \theta_w m_Z^2} \left[ \sum_X (g_{Zee}^v + j g_{Zee}^a) \Gamma_h(p_h^2) + I_V \text{Im } \Gamma_h(p_h^2) \right] \quad (9)$$

$v = z;$

where

$$I_V = \int_{t^+ t^-}^h 2j (g_{Ztt}^a g_{Vtt}^a + g_{Ztt}^v g_{Vtt}^v) f m_Z^2 s - g_{Ztt}^a g_{Vtt}^v (ef - g\tilde{h}) (\tilde{h} - s) + g_{Ztt}^v g_{Vtt}^a [(ef - g\tilde{h}) m_Z^2 + g(f^2 - (\tilde{h} - s)^2 + m_Z^2 s)] +$$

$$R_V = 4 (p_+; p_+; p_-; p_-) g_{Ztt}^a [ \int_{tt} g_{Vtt}^v (\tilde{h} + m_V^2/s) \int_{tt} g_{Vtt}^a f ]$$

It was useful to adopt above the following CP-even and CP-odd quantities:

$$\begin{aligned} e &= (p_+ p_+) (p_- p_-) \\ f &= (p_+ p_+) (p_+ p_-) \\ g &= (p_+ p_+) (p_- p_-) \\ \tilde{h} &= (p_+ p_+) (p_+ p_-) \end{aligned} \quad (10)$$

The vector-boson propagators are defined as  $\Delta_V(s) = [s - m_V^2]^{-1}$ . For quark propagators the following notation has been used:

$$\int_{tt} = \int_{tt}^h (k + p_t)^2 + \int_{tt}^i (k + p_t)^2 \quad \int_{tt} = \int_{tt}^h (k + p_t)^2 - \int_{tt}^i (k + p_t)^2; \quad (11)$$

where  $\Delta_x(q^2) = [q^2 - m_x^2]^{-1}$ . The vector and axial-vector couplings of the electron and of the top quark are summarized in the table below :

V	$g_{Vff}^v$	$g_{Vff}^a$
Z	$2T_3^f - 4Q^f \sin^2 \theta_w$	$2T_3^f$
	$4Q^f \sin \theta_w \cos \theta_w$	0

f	$T_3^f$	$Q^f$
e	$\frac{1}{2}$	1
t	$+\frac{1}{2}$	$+\frac{2}{3}$

The contribution proportional to the real part of the Higgs propagator have been already published in the literature [5]. We have noticed two mistakes present in the published result [5]: factor 1=2 is missing in Eq.(12) and sign in front of the first term in Eq.(13) should be reversed.

It has been argued in Ref. [5] that the contribution from the imaginary part of the Higgs propagator should be omitted since it is of higher order as being proportional to the Higgs width  $\Gamma_h$ . However, one should have in mind that the integration over the phase space around the Higgs-boson mass provides an extra factor  $\Gamma_h^{-1}$  which cancels  $\Gamma_h$  from the numerator of the imaginary part of the propagator leading to the contribution of the same order as the one proportional to the real part. This is exactly the same mechanism which is responsible for the applicability of the narrow width approximation. However, to generate the compensating factor  $\Gamma_h^{-1}$  it is necessary to have the pole of the Higgs-boson propagator with its vicinity (of the size of the  $\Gamma_h$ ) within the integration region. In the process under consideration, the square of the Higgs boson momentum,  $p_h^2 = (p_+ + p_-)^2$  is limited by  $4m_t^2$  and  $s - m_Z^2$ . It is easy to find that the position in the middle of the allowed region corresponds to  $m_h = 430$  and  $750$  GeV for  $\sqrt{s} = \sqrt{5}$  and  $1$  TeV, respectively. Since both for  $430$  GeV and  $750$  GeV the allowed region contains the

Higgs-boson pole with its vicinity of the size of the width one can expect contributions of the same order from both real and imaginary parts of the Higgs-boson propagator. We have found that the effect of the imaginary part could increase  $\sigma_{CP\text{-odd}}(CP\text{-mix } 1)$  even by 200%, however for that case  $\sigma$  was still below 1. The only phenomenologically relevant case for which the imaginary part was important was  $\sigma_{SM}(CP\text{-mix } 2)$  for  $M_h \approx 500$  GeV where we have found 10% increase caused by the imaginary part. It turns out that for all other considered cases the contribution from the imaginary part of the Higgs-boson propagator could be neglected for all practical purposes, although a consistent treatment demands both the real and imaginary contributions.

## References

- [1] T.D. Lee, Phys. Rev. D 8 (1973), 1226,  
G.C. Branco and M.N. Rebelo, Phys. Lett. B 160 (1985), 117,  
S. Weinberg, Phys. Rev. D 42 (1990), 860.
- [2] A. Pilaftsis, Phys. Lett. B 435 (1998), 88, Phys. Rev. D 58 (1998), 096010;  
A. Pilaftsis and C.E.M. Wagner, hep-ph/9902371;  
D.A. Demir, hep-ph/9901389.
- [3] K. Hagiwara, H. Murayama and I. Watanabe, Nucl. Phys. B 367 (1991), 257.
- [4] R. Brinkmann, Talk presented at ECFA/DESY Linear Collider Workshop 2nd ECFA/DESY Study on Physics and Detectors for a Linear Electron-Positron Collider, LAL, Orsay, France, April 5-7, 1998.
- [5] D. Atwood and A. Soni, Phys. Lett. B 419 (1998), 340.
- [6] J.F. Gunion, B. Grzadkowski and X.-G. He, Phys. Rev. Lett. 77 (1996), 5172 (hep-ph-9605326).  
See also  
D. Atwood and A. Soni, Phys. Rev. D 45 (1992), 2405,  
M. Davier, L. Duot, F. Le Diberder and A. Rouge, Phys. Lett. B 306 (1993), 411,  
M. Diehl and O. Nachtmann, Z. Phys. C 62 (1994), 397,  
B. Grzadkowski and J.F. Gunion, Phys. Lett. B 350 (1995), 218 (hep-ph/9501339).
- [7] B. Grzadkowski, J.F. Gunion and J. Kalinowski, hep-ph/9902308, to appear in Phys. Rev. D.
- [8] [http://www-jlc.kek.jp/JLC\\_proposal-e.html](http://www-jlc.kek.jp/JLC_proposal-e.html)
- [9] B. Grzadkowski and Z. Hübner, Nucl. Phys. B 484 (1997), 17.